

MATHEMATICAL SCIENCES DEPARTMENT  
COLLEGE OF SCIENCES  
OLD DOMINION UNIVERSITY  
NORFOLK, VIRGINIA 23529

LANGLEY  
GRANT  
IN-36-CR  
217715  
148

COMPARISON OF LASER MODELS

By

John H. Heinbockel, Principal Investigator

N89-26220

Unclas  
0217715

Progress Report  
For the period ended May 15, 1989

G3/36

Prepared for  
National Aeronautics and Space Administration  
Langley Research Center  
Hampton, Virginia 23665

(NASA-CR-185390) COMPARISON OF LASER MODELS  
Progress Report, period ended 15 May 1989  
(Old Dominion Univ.) 14 p CSCI 20E

Under  
Research Grant NAG-1-757  
Dr. Robert C. Costen, Technical Monitor  
SSD-High Energy Science Branch

Submitted by the  
Old Dominion University Research Foundation  
P.O. Box 6369  
Norfolk, Virginia 23508-0369

June 1989

Progress Report Research Grant NAG-1-757

ODURF 176613

Comparison of Laser Models

**Notation.**

In this report the following notations will be used:

$$\begin{array}{ll} x_1 = [RI] & x_4 = [I_2] \\ x_2 = [R] & x_5 = [I^*] \\ x_3 = [R_2] & x_6 = [I] \\ & x_7 = [\rho] \end{array}$$

where  $[ ]$  denotes concentration and  $R$  is a perfluoride radical,  $I$  is iodine,  $I^*$  is an excited state of iodine, and  $\rho$  is the photon density.

**Oscillatory Model.**

The following is the unscaled version of the time varying chemical kinetics equations for the simulation of the iodine laser operation

$$\begin{aligned} \frac{dx_1}{dt} &= k_1 x_2 x_5 + k_2 x_2 x_6 - \psi_1 x_1 - k_4 x_1 x_2 \\ \frac{dx_2}{dt} &= -k_1 x_2 x_5 - k_2 x_2 x_6 - 2k_3 x_2^2 + \psi_1 x_1 - k_4 x_1 x_2 \\ \frac{dx_3}{dt} &= k_3 x_2^2 + k_4 x_1 x_2 \\ \frac{dx_4}{dt} &= c_1 x_1 x_5 x_6 + c_2 x_1 x_6^2 + c_3 x_4 x_5 x_6 - \psi_2 x_4 + c_4 x_4 x_6^2 \\ \frac{dx_5}{dt} &= -k_1 x_2 x_5 - c_1 x_1 x_5 x_6 - c_3 x_4 x_5 x_6 - Q_1 x_1 x_5 - Q_2 x_4 x_5 \\ &\quad - A x_5 + \psi_1 x_1 + 0.51 \psi_2 x_4 - \Gamma_{max} \\ \frac{dx_6}{dt} &= 1.49 \psi_2 x_4 + Q_1 x_1 x_5 + Q_2 x_4 x_5 + A x_5 - c_1 x_1 x_5 x_6 + \Gamma_{max} \\ &\quad + k_4 x_1 x_2 - 2c_2 x_1 x_6^2 - c_3 x_4 x_5 x_6 - k_2 x_2 x_6 - 2c_4 x_4 x_6^2 \\ \frac{dx_7}{dt} &= \sqrt{\frac{\pi}{2.77}} \left( \frac{L}{L_c} \right) \Gamma_{max} + \frac{\log(R_1 R_2)}{2 \left( \frac{L_c}{L} \right)} x_7 + 2 \left( \frac{0.18}{L_c} \right)^2 A x_5 \\ \text{where } \Gamma_{max} &= \frac{c x_7 (x_5 - \frac{1}{2} x_6)}{A_{00} + B_{00} x_1} \end{aligned}$$

The above equations are solved subject to the initial conditions

$$x_1(0) = P * (3.5E16) \quad \text{and} \quad x_i(0) = 0, \quad i = 2, \dots, 7$$

where  $P$  is the pressure in torr. The above system was solved using a variable step size Runge-Kutta-Fehlberg algorithm. The figures 1.1 through 1.4 illustrated a typical set of solution curves to the above system of differential equations. Note the violent oscillations which occur during start-up of the laser. These oscillations require that small step sizes be taken during the numerical integration process in order to achieve some desired degree of accuracy. The numerical method becomes unstable and the results are meaningless if too large a step size is selected. This is not an uncommon situation in trying to numerically solve chemical kinetic systems of equations.

### Nonoscillatory Model.

The inversion term  $[I^*] - \frac{1}{2}[I] = x_5 - \frac{1}{2}x_6$  which occurs in the  $\Gamma_{max}$  term as well as the equations which define the rate of change of  $[I^*] = x_5$  and  $[I] = x_6$ , is the term which causes the oscillations in the nonlinear system of coupled ordinary differential equations. Under quasi-steady state conditions we set the rate of change of this term equal to zero. That is we require that

$$\frac{d}{dt} \left( [I^*] - \frac{1}{2}[I] \right) = 0$$

and then solve for  $\Gamma_{max}$  which is then relabeled as  $(\Gamma_{max})_{ss}$ . We find that

$$(\Gamma_{max}) = -Ax_5 - Q_2x_4x_5 + \{2\psi_1x_1 - 0.47\psi_2x_4 - 2k_1x_2x_5 + k_2x_2x_6 - c_1x_1x_5x_6 + 2c_2x_1x_6^2 - c_3x_4x_5x_6 + 2c_4x_4x_6^2 - k_4x_1x_2\}/3$$

Initially the  $\Gamma_{max}$  term is removed from the above equations as it is assumed to be initially zero. As time increases,  $[I^*]$  and  $[I]$  build up and when the threshold condition is met we have

$$[I^*] - \frac{1}{2}[I] = -\frac{1}{2} \frac{\ln(R_1 R_2)}{\sqrt{(\pi/2.77)}} (L\sigma)^{-1} = I_{th}.$$

Here it is assumed that steady state conditions have been achieved and gains balance with losses. The above steady state value is substituted for  $\Gamma_{max}$ . In this way the oscillatory character of the solution is removed and the integration can be made to proceed at a much faster rate. The results from this second nonoscillatory model were generated by L. Stock and are presented in the figures 1.5, 1.6. Observe how the oscillatory character of the solutions has been removed. Also, as a check on the model, the values of the power output were compared for both models and both values were found to be in agreement. The figure 1.7 lists the values of the reaction rate coefficients used in both models.

Currently there are four models for the simulation of an iodine laser. These models can be described by:

1. A time dependent model which is given by the above set of coupled nonlinear differential equations which describe the chemical kinetics at a fixed point as a function of time  $t$ .
2. A quasi-steady state model whereby the  $\Gamma_{max}$  term is replaced by its steady state value. This model is also a time dependent model with much faster integration times.
3. A noncompressible model which solves the above system of differential equations as a function of distance  $z$  along the axis of the laser tube. This model is characterized by substituting a material derivative in place of the time derivatives in the above differential equations. For an assumed steady flow, we make the substitutions:

$$\frac{d}{dt}[\ ] = \frac{\partial[\ ]}{\partial t} + \frac{\partial[\ ]}{\partial z} \frac{dz}{dt}$$

and assume that  $\frac{dz}{dt} = \omega$  is a constant. The time dependence is removed by assuming steady state values. Problems of stiffness arise in the numerical integration of this system.

4. A compressible flow laser model which solves the above system of differential equations with the material derivative replacing the time derivatives. In addition to these equations there is added: (i) a continuity equation (ii) an equation of state (iii) a momentum equation and (iv) an energy equation.

The figures 1.8 illustrates power vs beam radius which was obtained from the model 4, above assuming a parabolic velocity profile. The figure 1.9 illustrated power vs reflectivity for various pumping distances along a 45cm laser tube.

Current research is being directed toward:

1. Parameter studies using the compressible flow laser model.
2. Development of a two pass amplifier model.
3. Solve system of equations describing operation of high power iodine MOPA (Master Oscillator Power Amplifier). These equations are derived from the Frantz-Nodvik Amplifier theory.

## REFERENCES

1. L.V. Stock, J.W.Wilson, R.J.DeYoung, A Model for the Kinetics of a Solar-pumped Long Path Laser Experiment., NASA Technical Memorandum 87668, May 1986.
2. J.W.Wilson, S.Raju, Y.J. Shiu, Solar-Simulator-Pumped Atomic Iodine Laser Kinetics, NASA Technical Paper 2182, August 1983.

ORIGINAL PAGE IS  
OF POOR QUALITY

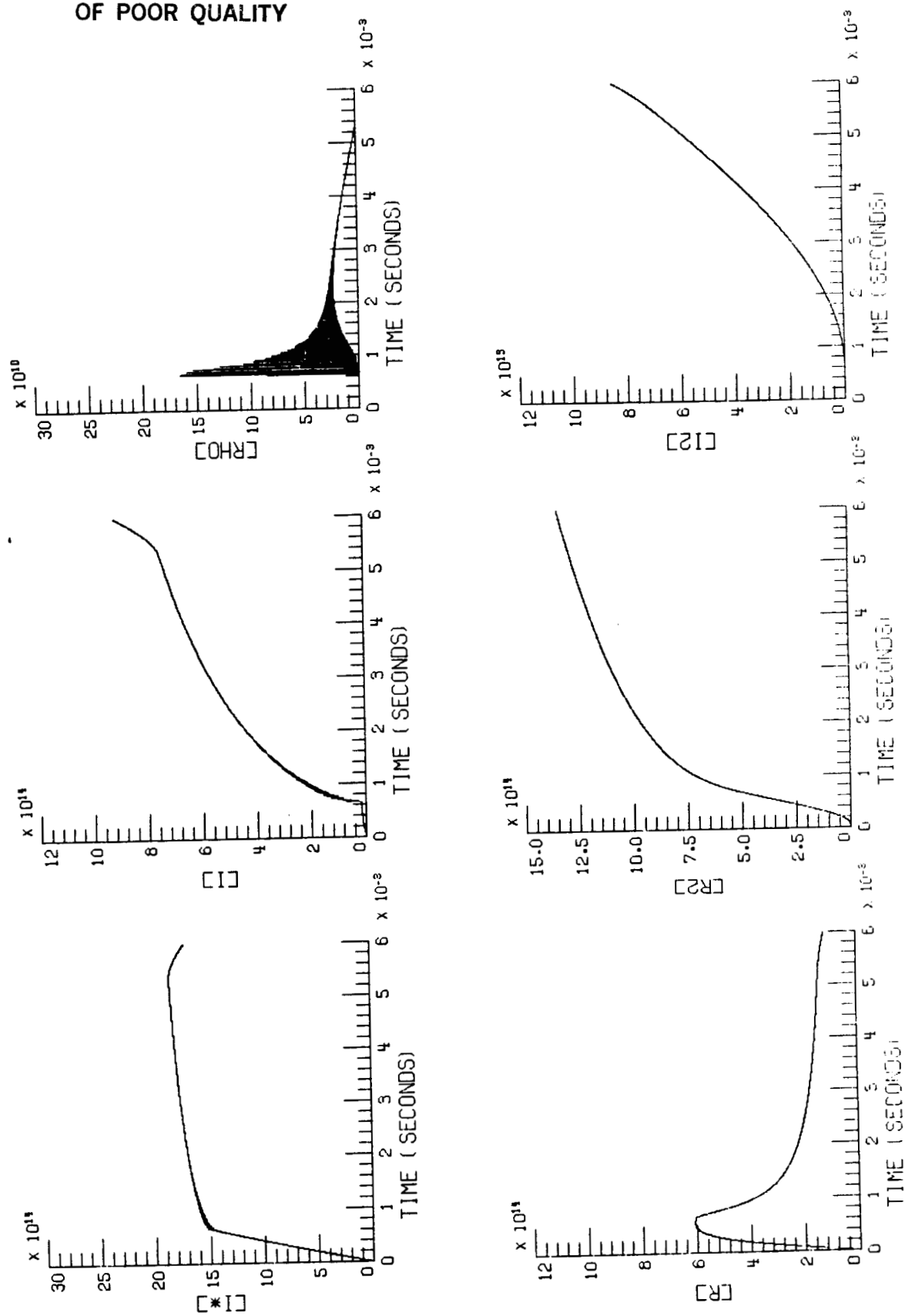


Fig. 1.1. Nominal Solution to Iodine Laser Equations.

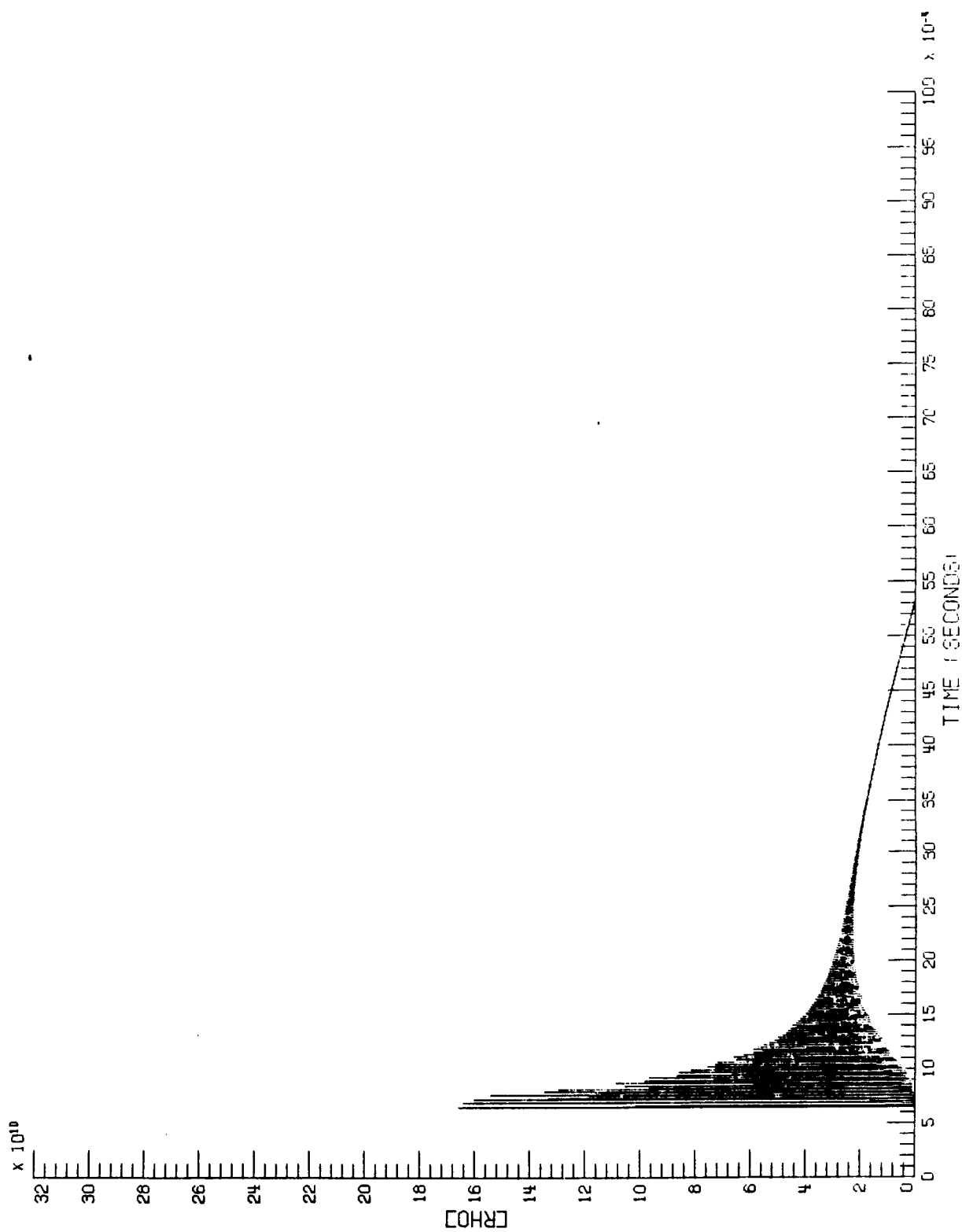


Fig. 1.2 Photon Density vs. Time

ORIGINAL PAGE IS  
OF POOR QUALITY

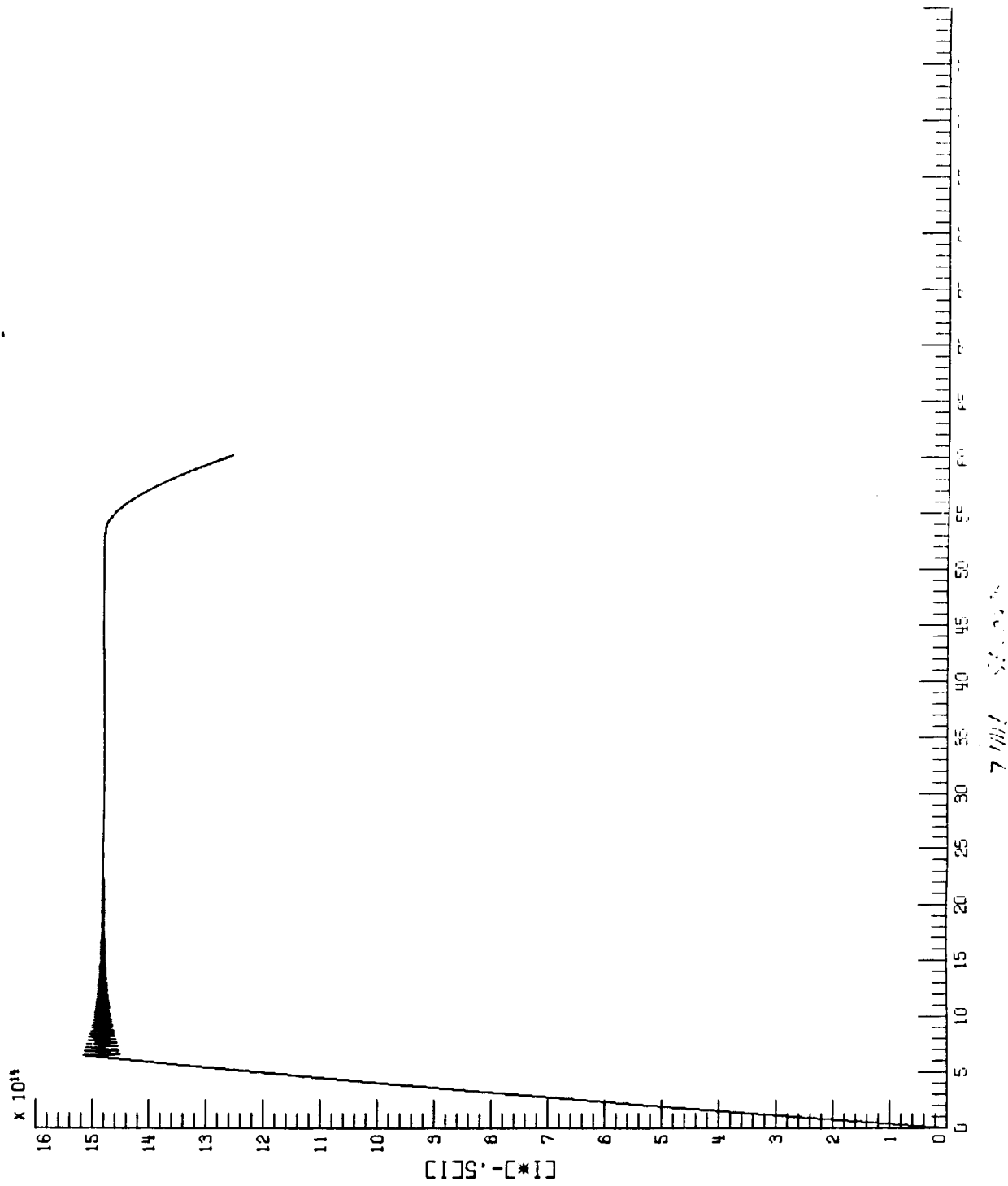


Fig. 1.3 Inversion Term vs. Time



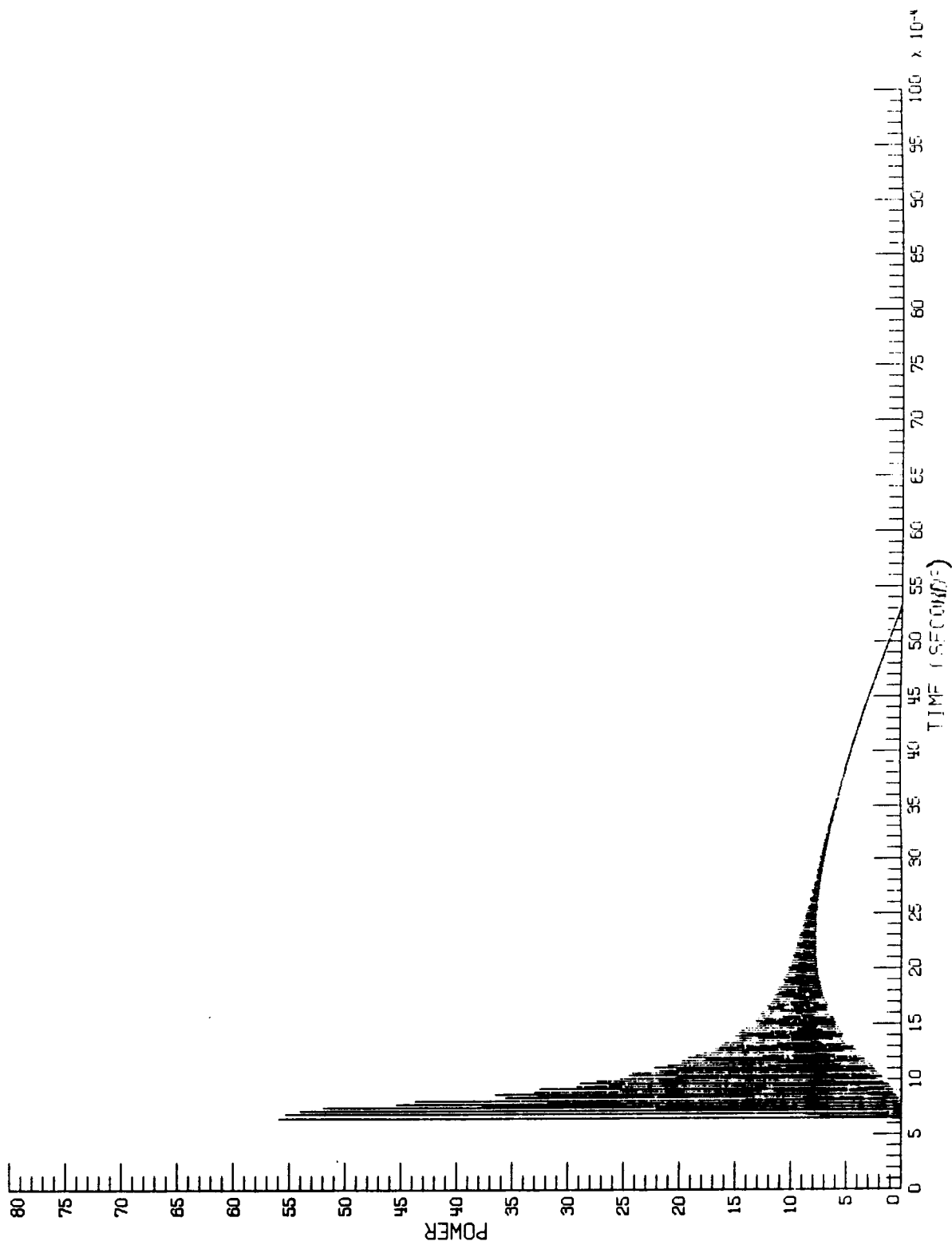


Fig. 1.4 Power vs. Time

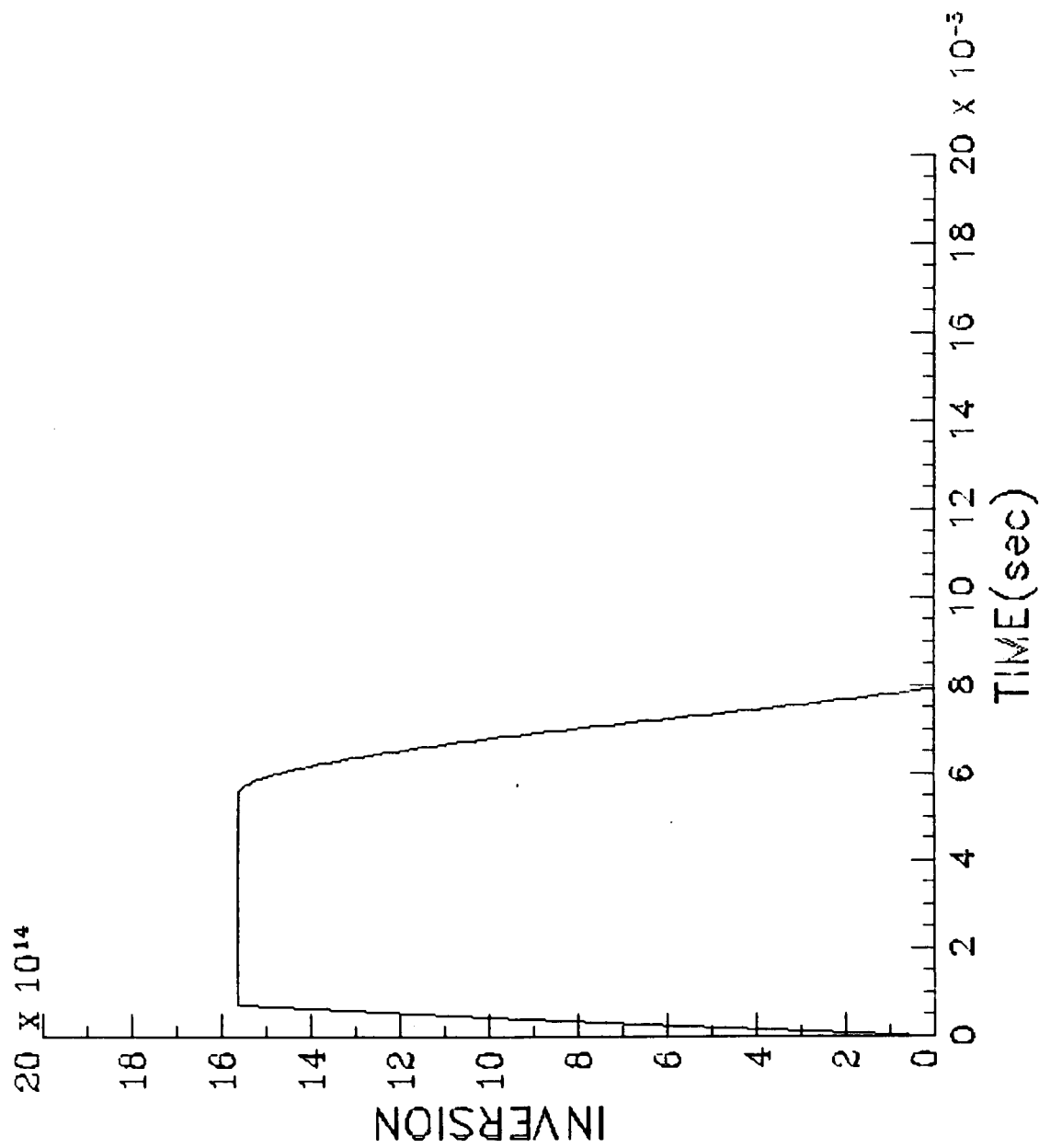


Fig. 1.5 Inversion vs. Time

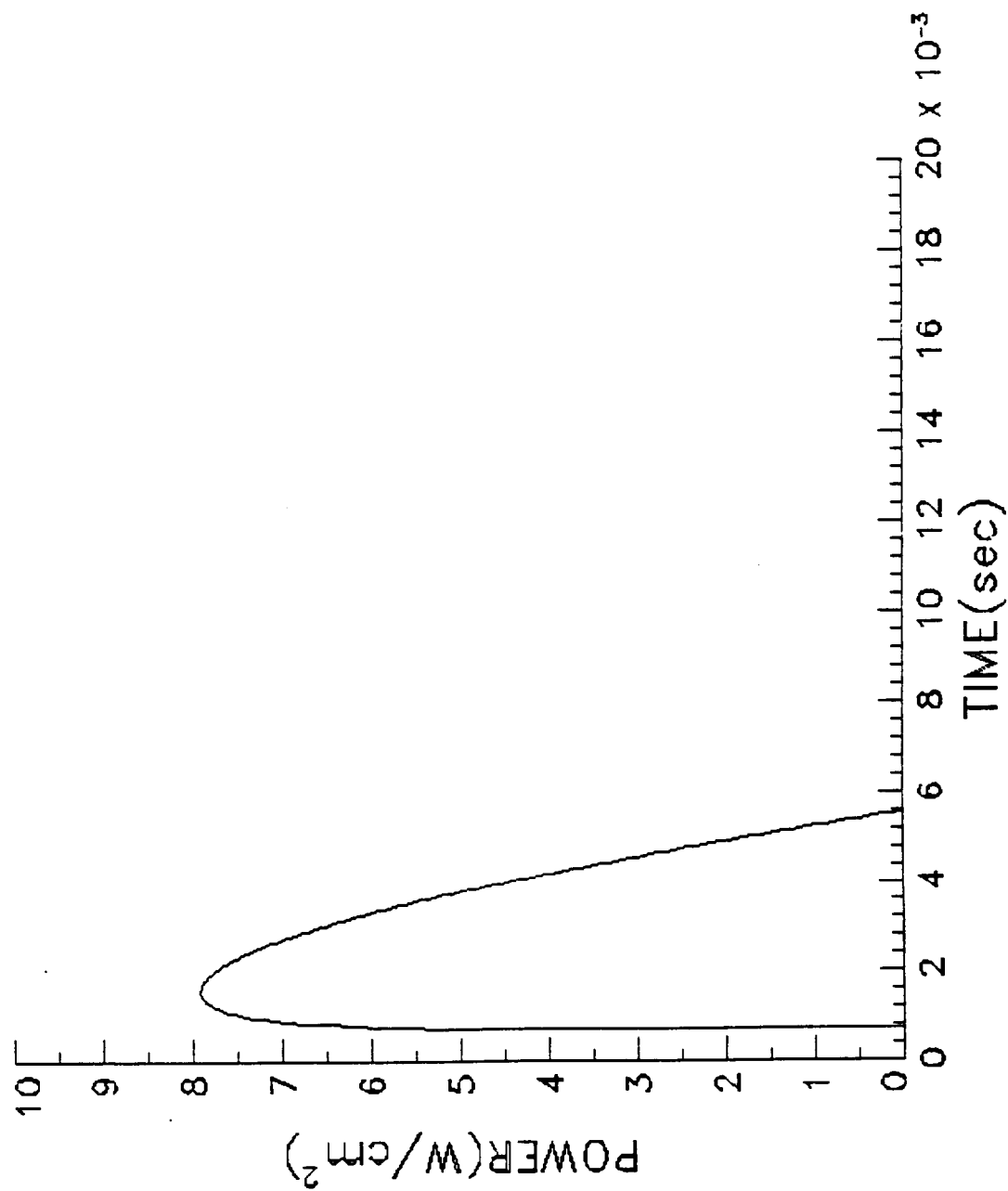


Fig. 1.6 Power vs. Time

TABLE I - Reaction rate coefficients and their associated reactions for the lasant  $n\text{-C}_3\text{F}_7\text{I}$  along with the parameters used to modify the optical time constant (ref. 2).

Lasant Reactions	$n\text{-C}_3\text{F}_7\text{I}$ Symbol	Reaction Rate Coefficient ( $\text{cm}^3$ )/sec
$\text{R} + \text{I}^* \rightarrow \text{RI}$	$\text{K}_1$	$.5600 \times 10^{-12}$
$\text{R} + \text{I} \rightarrow \text{RI}$	$\text{K}_2$	$.2300 \times 10^{-10}$
$\text{R} + \text{R} \rightarrow \text{R}_2$	$\text{K}_3$	$.2600 \times 10^{-11}$
$\text{R} + \text{RI} \rightarrow \text{R}_2 + \text{I}$	$\text{K}_4$	$.3000 \times 10^{-15}$
$\text{R} + \text{I}_2 \rightarrow \text{RI} + \text{I}$	$\text{K}_5$	$.0000 \times 10^{+00}$
$\text{I}^* + \text{I} + \text{RI} \rightarrow \text{I}_2 + \text{RI}$	$\text{C}_1$	$.3200 \times 10^{-32}$
$\text{I} + \text{I} + \text{RI} \rightarrow \text{I}_2 + \text{RI}$	$\text{C}_2$	$.8500 \times 10^{-31}$
$\text{I}^* + \text{I} + \text{I}_2 \rightarrow \text{I}_2 + \text{I}_2$	$\text{C}_3$	$.8000 \times 10^{-31}$
$\text{I} + \text{I} + \text{I}_2 \rightarrow \text{I}_2 + \text{I}_2$	$\text{C}_4$	$.3800 \times 10^{-29}$
$\text{I}^* + \text{RI} \rightarrow \text{I} + \text{RI}$	$\text{Q}_1$	$.2000 \times 10^{-18}$
$\text{I}^* + \text{I}_2 \rightarrow \text{I} + \text{I}_2$	$\text{Q}_2$	$.1900 \times 10^{-10}$
	$\text{T}_3$	1.0000
	$\alpha$	.0000

Fig. 1.7 Table I. Reaction Rate Coefficients

CFLM1-ADHN

$\omega = 10^3$

$R_1 = .9584792$

$C_{on} = 1,689 (10^3)$

$R_2 = .81634$

$Z_{oL} = 9.0 \text{ cm}$

$T_m = .147$

$L_c = 20. \text{ cm}$

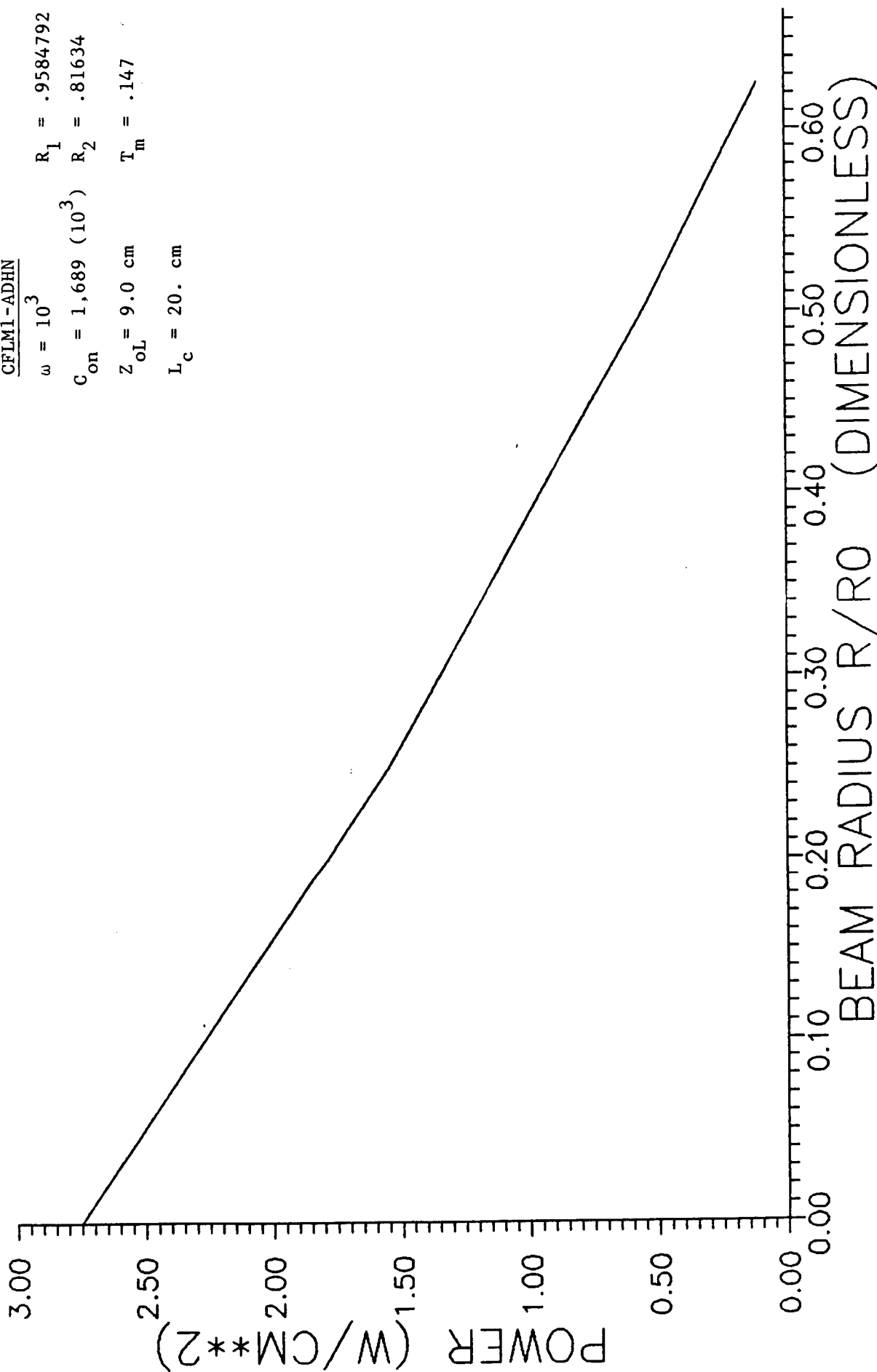


Fig. 1.8 Power vs. Beam Radius

# 45 CM LASER WITH VARIABLE PUMPING DISTANCE AND VARIABLE REFLECTIVITY

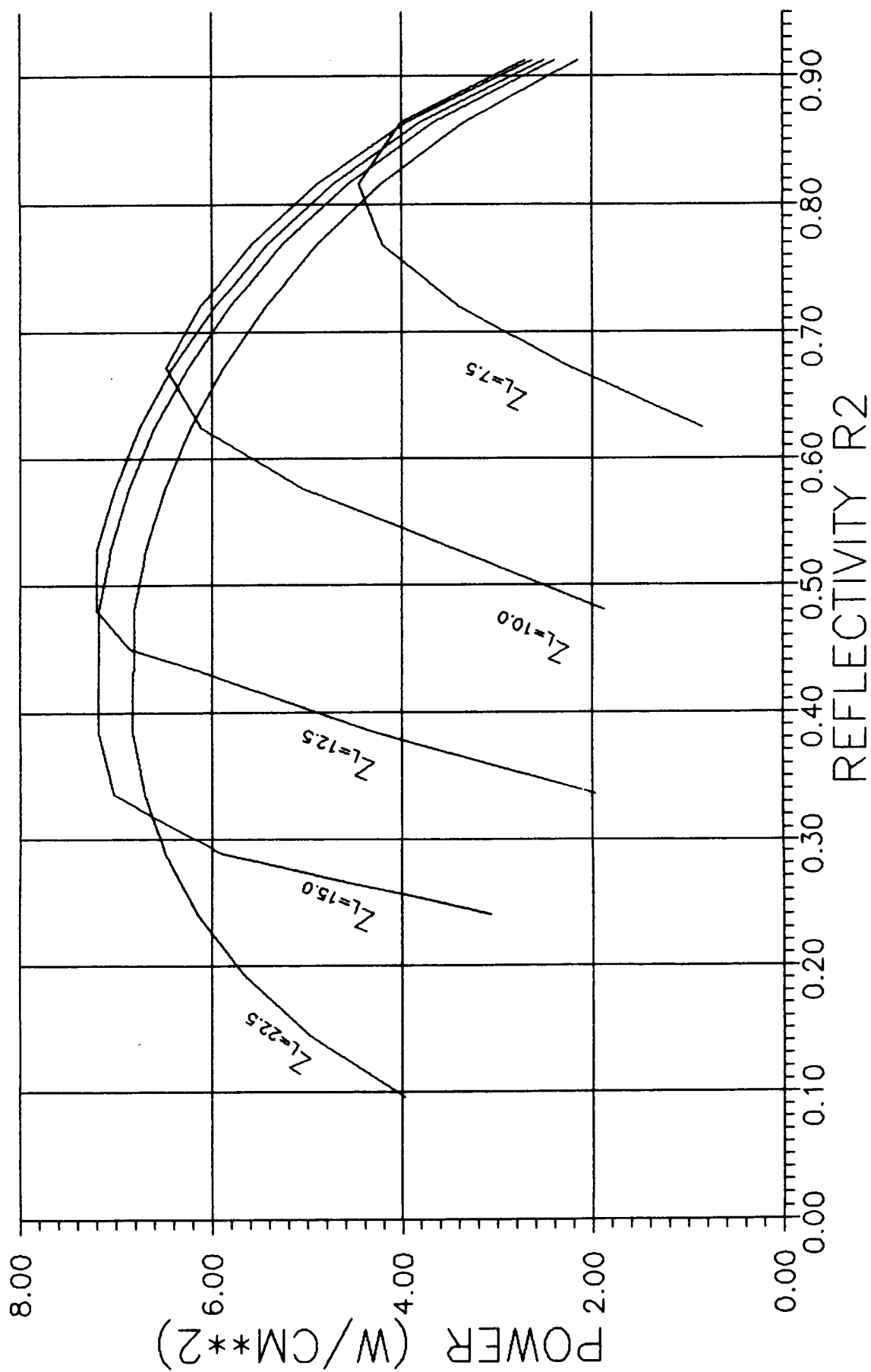


Fig. 1.9 Power vs. Reflectivity